Chip–Based Nanostructured Sensors Enable Accurate Identification and Classification of Circulating Tumor Cells in Prostate Cancer Patient Blood Samples

6 AUTHORS, INCLUDING:

Ivaylo Ivanov
University of Toronto
5 PUBLICATIONS   **28** CITATIONS

SEE PROFILE

Aleksandra Stanimirovic
University of Toronto
15 PUBLICATIONS   **644** CITATIONS

SEE PROFILE

Edward H Sargent
University of Toronto
418 PUBLICATIONS   **13,841** CITATIONS

SEE PROFILE

Shana O Kelley
University of Toronto
117 PUBLICATIONS   **3,914** CITATIONS

SEE PROFILE

Chip-Based Nanostructured Sensors Enable Accurate Identification and Classification of Circulating Tumor Cells in Prostate Cancer Patient Blood Samples

Ivaylo Ivanov,[†] Jessica Stojcic,[‡] Aleksandra Stanimirovic,[‡] Edward Sargent,[§] Robert K. Nam,[‡] and Shana O. Kelley*[,†,‖]

[†]Department of Pharmaceutical Science, Leslie Dan Faculty of Pharmacy, [‡]Division of Urology, Sunnybrook Research Institute, [§]Department of Electrical and Computer Engineering, Faculty of Engineering, and [‖]Department of Biochemistry, Faculty of Medicine, University of Toronto, Toronto, Ontario, Canada M5S 3M2

S Supporting Information

ABSTRACT: The identification and analysis of circulating tumor cells (CTCs) is an important goal for the development of noninvasive cancer diagnosis. Here we describe a chip-based method using nanostructured microelectrodes and electrochemical readout that confirms the identity of isolated CTCs and successfully interrogates them for specific biomarkers. We successfully analyze and classify prostate tumor cells, first in cultured cells, and ultimately in a pilot study involving blood samples from 16 prostate cancer patients as well as additional healthy controls. In all cases, and for all biomarkers investigated, the novel chip-based assay produced results that agreed with polymerase chain reaction (PCR). The approach developed has a simple workflow and scalable multiplexing, which makes it ideal for further studies of CTC biomarkers.
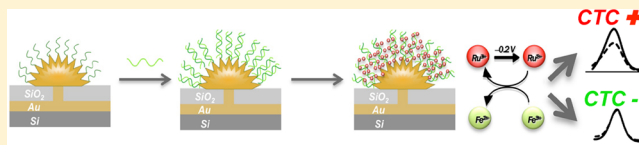
Circulating tumor cells (CTCs) are shed into the bloodstream as tumors grow and are believed to be the initiators of cancer spread. By colonizing sites distant from the primary tumor such as brain, liver, and bone, CTCs make cancer much more difficult to treat, and much more deadly. CTCs are found both in patients with primary tumors as well as metastatic disease, and it is of interest to understand the origins of CTCs at different stages of the disease.[1−8]

It is critically important to study the genetic makeup and other properties of CTCs to understand their role in cancer progression and to aid in the development of new treatments that would halt metastasis. In particular, understanding the significance of the presence of specific types of CTCs might lead to the eventual development of noninvasive cancer screening methods. For prostate cancer, where the widely used PSA test is falling out of favor, the analysis of CTCs could have significant clinical utility.

Monitoring CTCs is extremely challenging given the small numbers of CTCs found in a vast background of blood cells: they are outnumbered more than one-billion-fold by blood cells. A variety of methods have therefore been developed to capture CTCs from the bloodstream.[5,9] These include methods based on size[10−13] or the presence of surface antigens.[14−16] Several have employed microfluidic devices.[17−24]

Convenient methods of analyzing CTCs for specific biomarkers are much less developed than the aforesaid capture techniques. Research into the significance of specific biomarkers has been enabled by the polymerase chain reaction (PCR) and sequencing.[25,26] However, these methods do not offer a convenient, rapid, and low-cost path to translation toward clinical applications; and they are also prone to false positives in cases in which sample collection is not properly handled.

Ideally, a technique for translation to the clinic would rely on an automated, chip-based technique offering a high degree of biomarker multiplexing that would enable panels of a number of biomarkers to be reported on. Such tools would also promote the development of a comprehensive understanding of the biomarker profiles of CTCs on a patient-by-patient basis.

We present herein a new approach to CTC analysis (Figure 1) that relies on a class of chip-based electrochemical sensors. These sensors produce electrochemical signals that correspond to the presence of specific nucleic acid sequences.[31] The platform was previously shown to be effective in the detection of microRNAs in head-and-neck cancer cell lines,[27] infectious disease markers in bacterial lysates,[28] and cancer biomarkers in leukemia cells[29] and also in prostate solid tumor samples.[30] Here, we show that it is highly effective when challenged with RNA isolated from prostate cancer patient blood samples.

Our CTC chip analyzes a number of RNA sequences of interest from isolated CTCs. The samples are profiled both for markers that confirm their identify as CTCs and markers that may enable subtyping of prostate tumors.[3,7] A simple three-step workflow is described that streamlines that analysis of multiple markers within a single patient sample.
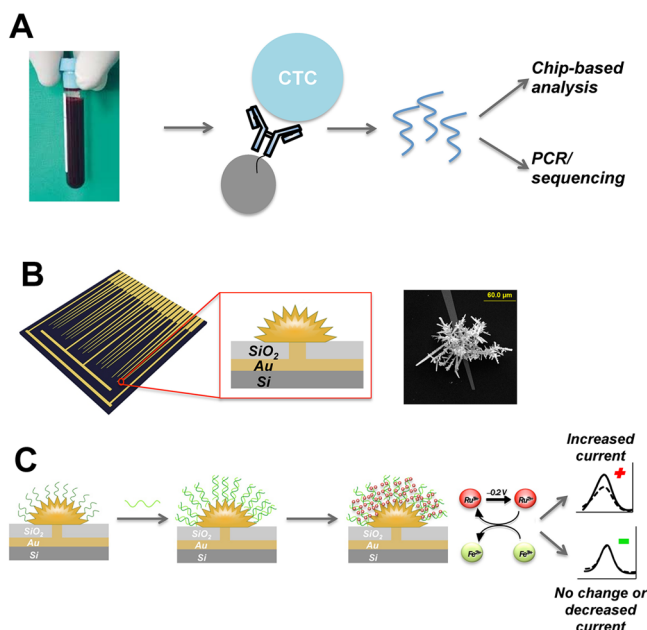
Figure 1. CTC analysis strategy: (A) CTCs are isolated from blood samples using a method employing magnetic beads, and RNA is then isolated. Samples are analyzed using chip-based sensors and PCR for confirmation. (B) Sensor fabrication. Silicon chips patterned with gold contacts and leads are passivated with silicon dioxide, and 5 μm apertures are produced at the ends of each lead. Gold electrodeposition is then used to produce fractal microelectrodes, and a nanostructured coating of palladium is then applied. (C) Sensors are coated with thiolated probes molecules, and then the binding of a target nucleic acid molecule increases the negative charge of the sensor. The accumulation of $Ru(NH_3)_6^{3+}$ generates an electrochemical signal that is amplified by $Fe(CN)_6^{3-}$. An increase in current indicates that the target sequence is present, while a constant current indicates that the sequence is absent.

EXPERIMENTAL SECTION

Chip Fabrication. Integrated biosensor circuits were fabricated by first passivating silicon wafer substrates with a thick thermally grown silicon dioxide layer. Positive photoresist was patterned to the desired electrical contact and lead structure using standard photolithographic methods. Subsequently, a 500 nm gold layer was deposited using electron-beam assisted gold evaporation, and a standard lift-off process was used to expose the desired electrical contacts and interconnects. Next, a second layer of 500 nm silicon dioxide was deposited to passivate the interconnects using chemical vapor deposition. Finally, 5 μm apertures were etched into the second passivating silicon dioxide layer, exposing the gold layer at the contact terminal point of each interconnecting line.

Sensor Fabrication. Chips were washed by sonicating in acetone for 5 min and rinsing with IPA and water. Nanostructured microelectrodes (NMEs) were electroplated using a standard three-electrode system consisting of a Ag/AgCl reference, a Pt auxiliary, and a 5 μm aperture Au working electrode. An electroplating solution containing 20 mM $HAuCl_4$ in 0.5 M HCl was used. NMEs were plated on the chip using an applied potential of 0 mV for 300 s. For finely nanostructured overlayer, a second electroplating solution was used (5 mM H_2PdCl_4 in 0.5 M $HClO_4$). The second electroplating was performed with an applied potential of −250 mV for 10 s.

Synthesis and Purification of PNA Probes. PNA probes were synthesized in house using a Protein Technologies Prelude peptide synthesizer. The following probe sequences are specific to PSA mRNA and TMP/ERG Type III mRNA: (P1) TMPRSS/ERG Type III probe (NH$_2$-C-G-ata-agg-ctt-cct-gcc-gcg-ct-CONH$_2$) and (P12) PSA (NH$_2$-C-G-D-gtc-att-gga-aat-aac-atg-gag-D-CONH$_2$). After the synthesis, the probes were purified using HPLC. Probe concentration was determined using a NanoDrop instrument.

Functionalizing the NMEs with PNA Probes. A solution of 100 nM PNA probe in 0.3× PBS was deposited on the NMEs surface in a dark humidity chamber overnight at RT.

Electrochemical Detection of Hybridization of the mRNA Target with PNA Probes. Electrochemical measurements were made using an Epsilon potentiostat. After probe deposition, unbound probe was removed by washing at 37 °C for 30 min and twice at room temperature for 5 min. The background signal (from the probe) was scanned in electrocatalytic solution (10 μM $Ru(NH_3)_6^{3+}$ and 1 mM $Fe(CN)_6^{3-}$) in PBS. NMEs were incubated with purified total RNA, from cultured cells or CTCs, diluted with 0.3× PBS, at 37 °C for 1 h. After hybridization, the chips were washed twice with 0.3× PBS at RT for 5 min. The same catalytic solution was used for the chip scanning before and following hybridization.

RT-PCR. Total RNA (extracted with Trizol, Invitrogen) was used for cDNA synthesis with the First Strand DNA synthesis kit (Invitrogen) and Superscript III reverse transcriptase and random hexamers according the manufacturer's protocol. A volume of 2 μLof cDNA were then used in a 50 μL PCR reaction with 1 μL of 100 μM gene specific primers (specific to TMP/ERG Type III gene fusion and PSA gene). The two PCR primer-pairs were designed to have an annealing temperature of 57 °C, which allows one RNA sample to be tested for TMP/ERG Type III mRNA and PSA mRNA at the same time. The PCR program was as follows: template denaturing at 94 °C for 3 min followed by 35 cycles of template denaturing at 95 °C for 30 s and primer annealing at 57 °C for 30 s and DNA chain extension at 72 °C for 1 min. The PCR reaction was then incubated at 72 °C for a further 10 min. The PCR products were visualized using agarose gel electrophoresis.

PCR primers for TMPRSS/ERG Type III gene fusion (600 bp PCR product)

Forward primer: TFP (5′-cag-gag-gcg-gag-gcg-ga-3′)

Reverse primer: TRP (5′-ggc-gtt-gta-gct-ggg-ggt-gag-3′)

PCR primers for PSA gene (500 bp PCR product)

Forward primer: FPPSA1 (5′-ttg-tgg-gag-gct-ggg-agt-g-3′)

Reverse primer: RPPSA1 (5′-cct-tct-gag-ggt-gaa-ctt-gcg-3′)

Asymmetric PCR. TMP/ERG Type III ssDNA and PSA ssDNA were synthesized by asymmetric PCR and used as positive controls for electrochemical detection of mRNA on a chip. TMP/ERG Type III ssDNA was synthesized in a 50 μL reaction using 10 ng of PCR4TOPO-TMP/ERG Type III plasmid vector (contains inserted TMP/ERG Type III gene fusion) template, 1 μL of 100 μM forward primer (TFP), and 1 μL of 1 μM reverse primer (TRP). The PCR program was as follows: template denaturing at 94 °C for 3 min, followed by 40 cycles of template denaturing at 95 °C for 30 s, primer annealing at 60 °C for 30 s, and DNA extension at 72 °C for 1 min. The PCR reaction was then incubated at 72 °C for

another 10 min. For PSA ssDNA synthesis, the same PCR program was used but different primers were required for efficient amplification. In total, 10 ng of PSA-PCR product (obtained by conventional PCR) in a 50 μL reaction was used as a template. As a forward primer, 1 μL of 60 μM FPPSA5 was used, and as a reverse primer 1 μL of 3 μM RPPSA2 was used. The primer-pair annealing temperature was 65 °C.

Primers for TMPRSS/ERG Type III gene fusion (600 nt ssDNA product)

    Forward primer: TFP (5′-cag-gag-gcg-gag-gcg-ga-3′)

    Reverse primer: TRP (5′-ggc-gtt-gta-gct-ggg-ggt-gag-3′)

Primers for PSA gene (200 nt ssDNA product)

    Forward primer: FPPSA5 (5′-gat-gac-tcc-agc-cac-gac-3′)

    Reverse primer: RPPSA2 (5′-gtc-att-gga-aat-aac-atg-gag-gtc-c-3′)

For preparative purification of ssDNA, four PCR reactions were pooled together and DNA was precipitated with ethanol. Then the desired ssDNA was separated from dsDNA by agarose gel electrophoresis. Only the ssDNA was excised from the gel and further purified with a PCR clean up kit (Promega). The ssDNA was eluted, from the column, with 50 μL of water, and the concentration was estimated by using a NanoDrop instrument. To confirm the identity of ssDNA, restriction analysis was used together with NaOH-denaturing agarose gel electrophoresis.

Patient Selection and Consent Protocol. To maximize the ability to detect CTCs from the patient samples, we selected three groups of patients over a 2 year period: (1) patients presenting with metastatic prostate cancer at diagnosis (n = 6); (2) patients undergoing radical prostatectomy treatment for clinically localized prostate cancer (n = 9); and (3) a control group with no evidence of cancer proven by prostate biopsy (n = 2). All blood samples were collected with consent prior to prostate biopsy or radical prostatectomy. The characteristics of these patients are outlined in Table S1 in the Supporting Information.

CTCs Purification from Patient Blood Samples and RNA Extraction. CTCs were purified from patient blood samples using the Miltenyi Biotec (MACS) method.[14] Blood samples (10 mL) were diluted with MACS PBS pH 4.2 (contains 2 mM EDTA and 0.5% BSA) and fractionated by Ficoll gradient centrifugation at 400g for 40 min at 20 °C. The CTCs were collected from the interphase (between the Ficoll layer and the plasma) and further purified from the blood cells using EpCAM magnetic microbeads (CD326, human) and MS columns. Finally, the CTCs were eluted from the column with 1 mL of MACS PBS and centrifuged at 200g for 10 min at 4 °C. The supernatant was discarded, and the CTCs were lysed with 0.8 mL of Trizol (Invitrogen) for further RNA extraction.

■ RESULTS AND DISCUSSION

Sensor Design and Readout Strategy. The sensors used in this study are produced using a combination of top-down and bottom-up microfabrication (Figure 1B). Using photolithography, a pattern of contacts and leads are produced on silicon. This pattern is then passivated with a top layer of SiO_2, and then small (5 μm) circular apertures are opened at the end of each lead. These apertures are then used to template the growth of electrodeposited gold sensors. The choice of deposition and solution conditions can be used to control the size and surface morphology of the sensor.[32,35] Previous studies

of these sensors have confirmed that they enable highly reproducible and sensitive detection of nucleic acids analytes.

In this study, we sought to generate sensors with very low detection limits to meet the objective of analyzing the small numbers of CTCs present in patient samples. The sensors generated were therefore made to extend fully 100 μm into solution to facilitate collisions with slow-moving mRNAs.[35] In addition, they were covered with a fine coating of nanostructured palladium to enable efficient probe display.[33,34] The resultant nanostructured microelectrodes combine the advantage of enhanced collisional frequencies and high target capture efficiencies.[35]

The electrochemical reporter system used with these sensors[38] employs two different redox-active probes, Ru-$(NH_3)_6^{3+}$ and $Fe(CN)_6^{3-}$ (Figure 1C). The Ru(II) species accumulates at the sensor surface in proportion with the hybridization of negatively charged nucleic acid target molecules to the NME-tethered probes and is reduced when a potential of −0.175 V (vs Ag/AgCl) is applied to the sensors. The Fe(III) species is repelled from the sensor surface because it is anionic, but since it is more readily reduced than $Ru(NH_3)_6^{3+}$, it is able to oxidize the reduced ruthenium and regenerate it for further electrochemical cycles. This electrocatalytic approach provides signal amplification and is particularly effective with nanostructured surfaces.[36,37]

Development of Probes for CTC-Specific Markers. To obtain proof-of-concept for the use of these sensors for CTC analysis, two probe molecules were designed that would (1) establish the identity of prostate-tumor derived CTCs and (2) report of the presence of a prostate-tumor specific biomarker. A marker unique to the prostate, the prostate-specific antigen (PSA) mRNA, was selected to enable unambiguous confirmation that the collected bloodborne cells originate from a prostate tumor. Another marker found in a subset of prostate tumors, the TMPRSS2-ERG Type III gene fusion, was selected in view of studies indicating that it may offer information relevant to the classification of different types of prostate tumors.[39] Probes against PSA and TMPRSS2-ERG were designed to be highly specific to these mRNAs even in the presence of the other RNAs found in human cells. These probes were made as peptide nucleic acids to ensure maximum sensitivity[29] and featured a thiol on the PNA terminus to provide a linkage site to the palladium-coated sensor.

The sensor-bound probes were validated using targets produced by asymmetric PCR of a template containing the sequence complementary to the PSA mRNA and the TMPRSS2-ERG mRNA (Figure 2). The targets were 200 nucleotides for PSA and 600 nucleotides for TMPRSS2-ERG. Several concentrations were tested, and at concentrations as low as 1 pg/μL, statistically significant changes in current were observed, indicating that the sensors exhibited sensitivity toward these targets in the low picomolar concentration range.

The sensors were then challenged with different cultured prostate cancer cell lines to assess whether they were sufficiently sensitive to investigate the small number of CTCs found in patients (Figure 3). Using as few as 100 cells in 40 μL, sensors modified with probes against the PSA mRNA and the TMPRSS2-ERG mRNA exhibited a statistically significant signal change. Given that the sample volume used in these trials could be reduced by ∼10-fold, this indicates that the system was capable of analyzing the very low numbers of CTCs typically found in prostate cancer patients. It is noteworthy that higher background levels were noted with the TMPRSS2-ERG
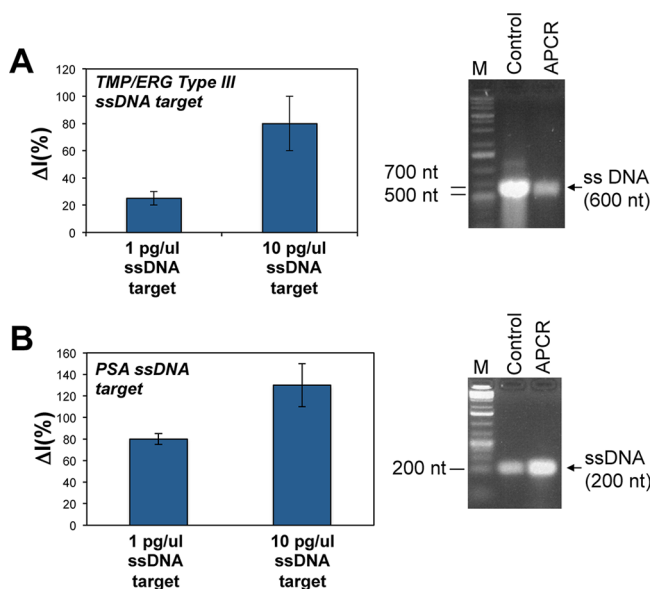
400

dx.doi.org/10.1021/ac3029739 | Anal. Chem. 2013, 85, 398−403

Figure 2. Validation of probe for CTC markers using asymmetric PCR products. The sensitivity of the probes to large biomarkers (mRNAs) was validated using ssDNA targets synthesized by asymmetric PCR. Two different concentrations of targets (1 and 10 pg/μL) were used to test how the signal changes with increasing the concentration of targets. The figure shows an electrochemical detection of ssDNA targets, using TMP/ERG Type III biosensor (A) or PSA biosensor (B). To confirm the size and integrity of the ssDNA targets, denaturing gel electrophoresis were used.

sensors relative to the PSA sensors, which likely relates to the fact that DU145 cells do not express PSA, but they do express the wild-type genes that could interact with the TMPRSS2-ERG sensors. A PCR assay was also developed and optimized for PSA and the TMPRSS2-ERG type III gene fusion and was found to have a similar limit of detection. This method did not show any background levels for the DU145 cells, because the PCR primers used do not target the fusion site. While crosstalk of WT mRNAs with fusion probes is a limitation of hybridization-based approaches like the one described here, the fact that the fusion site is probed directly increases the overall specificity of the assay because PCR can have difficulty identifying specific fusion sequences.

Analysis of Patient Samples. A pilot study analyzing CTCs in blood samples from prostate cancer patients was then conducted to examine the potential clinical relevance of the methodology developed (Figure 4). A set of 16 patients with high PSA levels was selected for the study (Table S1 in the Supporting Information), and 10 mL blood samples were drawn with consent. CTCs were isolated using magnetic beads, and RNA was purified from the isolated cells (see Figure S1 in the Supporting Information for validation of sample preparation using a commercial kit). Blood from a healthy donor was also processed the same way and analyzed. The RNA samples were analyzed using the PSA/TMPRSS2-ERG chips, and the chip results are summarized in Figure 4. The healthy donor blood did not produce appreciable signal changes at the sensors, and in addition, two patients that were later found to be biopsy-negative for prostate cancer were negative when analyzed with the chip-based sensors. For 9 of the 16 patient samples tested, significant signal changes at the anti-PSA sensors were observed. The highest signals were obtained with patient samples where the biopsies were assigned high Gleason
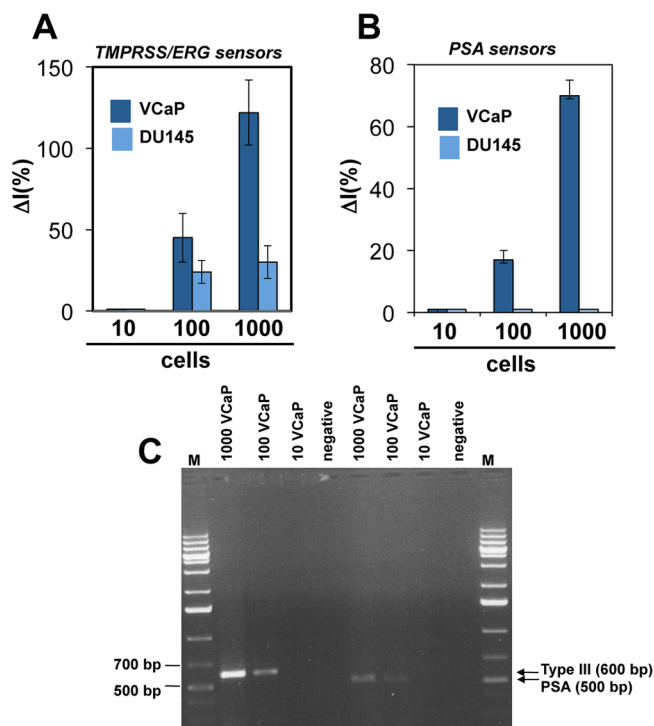

Figure 3. Analysis of DU145 and VCaP cells. VCaP cells express the selected biomarkers (PSA gene and TMP/ERG Type III gene fusion) and were used as a positive control for the detection of mRNA, on a chip. As a negative control, we used DU145 cells, which do not express the selected biomarkers. Electrochemical detection of TMP/ERG Type III mRNA (A) and PSA mRNA (B) used three different RNA concentrations, corresponding to 1000, 100, and 10 cells. (C) RT-PCR using RNA extracted from 1000, 100, and 10 VCaP cells. The limit of mRNA detection for both NMEs and RT-PCR is between 10 and 100 VCaP cells.

scores. For 2 of the 15 samples, increased current was observed at the anti-TMPRSS2-ERG sensors. In each case, PCR was used to confirm the presence or absence of the PSA mRNA and TMPRSS2-ERG type III mRNA, and the identical results were obtained. The PCR product from one of the TMPRSS2-ERG positive samples was sequenced, and the correct sequence of the type III fusion was obtained (Figure S2 in the Supporting Information).

It is noteworthy that, using both the PCR gold-standard assay and also the novel chip-based assay, there were certain patient samples, even ones where the corresponding biopsies had yielded high Gleason scores, in which CTCs were not detectable. This may reflect a lack of CTCs in these samples or inefficiencies in the sample preparation strategy that was employed. Future efforts will explore different cell capture methods to determine whether CTC screening could be used to identify all patients who are identified by biopsy.

While limited multiplexing was used in this study, the chip-based detection strategy has scalable multiplexing that could be employed to analyze much larger panels of markers. Future efforts will leverage this capability to provide more information-rich analyses of CTCs.

These results indicate that a chip-based strategy for molecular detection successfully enables screening of patient blood samples for CTC markers. The method produces results that are consistent with established PCR-based techniques. It is the first alternative to PCR ever documented to accurately
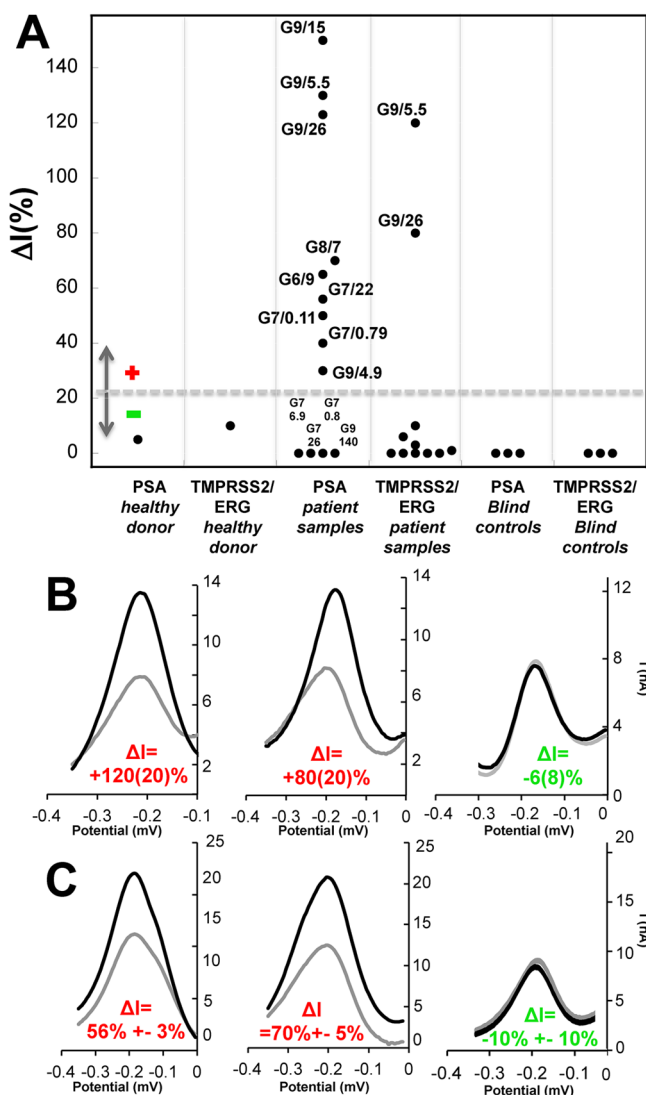
Figure 4. Analysis of patient samples for CTCs. (A) Compilation of patient data showing changes in current measured at sensors functionalized with probes against the PSA mRNA and TMPRSS2-ERG type III mRNA. Gleason Scores and PSA levels are shown next to each data point. ΔI values that were negative were assigned zero current; (B) representative differential pulse voltammograms from TMPRSS2-ERG sensors; (C) representative differential pulse voltammograms from PSA sensors.

identify CTC-positive samples. Using a simple, 3-step work-flow, the presence of CTCs was confirmed and a specific prostate cancer biomarker was also assessed in each patient sample. Future work will extend this system to also include in-line CTC capture for a fully integrated solution to CTC capture and analysis.

CONCLUSIONS

Circulating tumor cells are an important class of circulating cancer markers that may enable noninvasive diagnosis and contain molecular-level information guiding treatment. They are challenging to analyze given their low levels even in large patient samples, and few methods have been developed for their analysis. We have described an effective method that allows CTC markers to be analyzed that relies on a multiplexed sensor chip. This method is inherently scalable and could enable the screening of large panels of markers in CTCs to

advance our understanding of CTC biology and the value of these cells as diagnostic and prognostic markers.

ASSOCIATED CONTENT

Ⓢ Supporting Information

CTC capture efficiency trials (Figure S1), PCR trials showing equivalency with the chip-based analysis (Figure S2), and patient information (Table S1). This material is available free of charge via the Internet at http://pubs.acs.org.

AUTHOR INFORMATION

Corresponding Author
*E-mail: shana.kelley@utoronto.ca.

Notes
The authors declare no competing financial interest.

ACKNOWLEDGMENTS

REFERENCES

(1) Danila, D. C.; Pantel, K.; Fleisher, M.; Scher, H. I. *Cancer J.* **2011**, *17*, 438−450.

(2) Bednarz-Knoll, N.; Alix-Panabieres, C.; Pantel, K. *Breast Cancer Res.* **2011**, *13*, 228.

(3) Armstrong, A. J.; Eisenberger, M. A.; Halabi, S.; Oudard, S.; Nanus, D. M.; Petrilak, D. P.; Sartor, A. O.; Scher, H. I. *Eur. Urol.* **2012**, *61*, 549−559.

(4) Alix-Panabieres, C.; Schwarzenbach, H.; Pantel, K. *Annu. Rev. Med.* **2012**, *63*, 199−215.

(5) Mikulova, V.; Kolostova, K.; Zima, J. *Folia. Biol. (Praha)* **2012**, *57*, 151−161.

(6) Yu, J. Q.; Cristofanilli, M. *J. Nucl. Med.* **2011**, *52*, 1501−1504.

(7) Danila, D. C.; Flesher, M.; Scher, H. I. *Clin. Cancer Res.* **2011**, *17*, 3903−3912.

(8) Doyen, J.; Alix-Panabieres, C.; Hofman, P.; Parks, S. K.; Chamorey, E.; Naman, H.; Hannoun-Levi, J. M. *Crit. Rev. Oncol. Hematol.* **2012**, *81*, 241−256.

(9) Yu, M.; Stott, S.; Toner, M.; Maheswaran, S.; Haber, D. A. *J. Cell Biol.* **2011**, *192*, 373−382.

(10) Roosenberg, R.; Gertler, R.; Friederichs, J.; Fueherer, K.; Dahm, M.; Phelp, R.; Thorban, S.; Nekarada, H.; Siewert, J. R. *Cytometry* **2002**, *49*, 150−158.

(11) Baker, M. K.; Mikhitarian, K.; Osta, W.; Callahan, K.; Hoda, R.; Brescia, F.; Kneuper-Hall, R.; Mitas, M.; Cole, D. J.; Gillanders, W. E. *Cancer Res.* **2003**, *9*, 4865−4871.

(12) Pinzani, P.; Salvadori, B.; Simi, L.; Bianchi, S.; Distante, V.; Cataliotti, L.; Pazzagli, M.; Orlando, C. *Hum. Pathol.* **2006**, *37*, 711−718.

(13) Vona, G.; Sabile, A.; Louha, M.; Sitruk, V.; Roman, S.; Schutze, K.; Capron, F.; Franco, D.; Pazzagi, M.; Vekemans, M.; Lacour, B.; Brechot, C.; Paterlini-Brechot, P. *Am. J. Pathol.* **2000**, *156*, 57−63.

(14) Miltemyi, S.; Muller, W.; Weichel, W.; Radbruch, A. *Cytometry* **1990**, *11*, 231−238.

(15) Rao, C. G.; Chianese, D.; Doyle, G. V.; Miller, M. C.; Russell, T.; Sanders, R. A., Jr.; Terstappem, L. W. *Int. J. Oncol.* **2005**, *27*, 49−57.

(16) Schmitt, M.; Foeksens, J. A. *Breast Cancer Res.* **2009**, *11*, 109.

(17) Talasat, A. H.; Powell, A. A.; Huber, D. E.; Berbee, J. G.; Roh, K. H.; Yu, W.; Davis, M. M.; Pease, R. F.; Mindrinos, M. N.; Jeffrey, S. S.; Davis, R. W. *Proc. Natl. Acad. Sci. U.S.A.* **2009**, *106*, 3970−3975.

402

dx.doi.org/10.1021/ac3029739 | *Anal. Chem.* 2013, 85, 398−403

(18) Shah, A. M.; Yu, M.; Nakamura, Z.; Ciciliano, J.; Ulman, M.; Kotz, K.; Stott, S. L.; Maheswaran, S.; Haber, D. A.; Toner, M. *Anal. Chem.* **2012**, *84*, 3682−3688.

(19) Watkins, N.; Irimia, D.; Toner, M.; Bashir, R. *IEEE Pulse* **2011**, *2*, 19−27.

(20) Stott, S. L.; Hsu, C. H.; Tsukrov, D. I.; Yu, M.; Miyamoto, D. T.; Waltman, B. A.; Rothenberg, S. M.; Shah, A. M.; Smas, M. E.; Korir, G. K.; Floyd, F. P., Jr.; Gilman, A. J.; Lord, J. B.; Winokur, D.; Springer, S.; Irimia, D.; Nagrath, S.; Sequist, L. V.; Lee, R. J.; Isselbacher, K. J.; Maheswaran, S.; Haber, D. A.; Toner, M. *Proc. Natl. Acad. Sci. U.S.A.* **2010**, *107*, 182−18397.

(21) Stott, S. L.; Lee, R. J.; Nagrath, S.; Yu, M.; Miyamoto, D. T.; Ulkus, L.; Inssera, E. J.; Ulman, M.; Springer, S.; Nakamura, Z.; Moore, A. L.; Tsukrov, D. I.; Kempner, M. E.; Dahl, D. M.; Wu, C. L.; Lafrate, A. J.; Smith, M. R.; Tompkins, R. G.; Sequist, L. V.; Toner, M.; Haber, D. A.; Maheswaran, S. *Sci. Transl. Med.* **2010**, *2*, 25ra23.

(22) Sequist, L. V.; Nagrath, S.; Toner, M.; Haber, D. A.; Lynch, T. J. *J. Thorac. Oncol.* **2009**, *4*, 218−283.

(23) Lobodasch, K.; Frohlich, F.; Rengsberger, M.; Schubert, R.; Dengler, R.; Pachman, U.; Pachman, K. *Breast* **2007**, *16*, 211−218.

(24) Pachman, K.; Camara, O.; Kavallaris, A.; Schneider, U.; Schunnemann, S.; Hoffken, K. *Breast Cancer Res.* **2005a**, *7*, R975−R979.

(25) Pantel, K.; Muller, V.; Auer, M.; Nusser, N.; Harbeck, N.; Braun, S. *Clin. Cancer Res.* **2003**, *9*, 6326−6334.

(26) Mitas, M.; Mikhitarian, K.; Walters, C.; Baron, P. L.; Elliott, B. M.; Brothers, T. E.; Robison, J. G.; Metcalf, J. S.; Palesch, Y. Y.; Zhang, Z.; Gillanders, W. E.; Cole, D. *J. Cancer* **2001**, *93*, 162−171.

(27) Yang, H.; Hui, A.; Pampalakis, G.; Soleymani, L.; Liu, F.-F.; Sargent, E. H.; Kelley, S. O. *Angew. Chem., Int. Ed.* **2009**, *48*, 8461−8464.

(28) Lam, B.; Fang, Z.; Sargent, E. H.; Kelley, S. O. *Anal. Chem.* **2012**, *84*, 21−25.

(29) Vasilyeva, E.; Lam, B.; Fang, Z.; Minden, M. D.; Sargent, E. H.; Kelley, S. O. *Angew. Chem.* **2011**, *50*, 4137−4141.

(30) Fang, Z.; Soleymani, L.; Pampalakis, G.; Yoshimoto, M.; Squire, J. A.; Sargent, E. H.; Kelley, S. O. *ACS Nano* **2009**, *3*, 3207−3213.

(31) Fang, Z.; Kelley, S. O. *Anal. Chem.* **2009**, *81*, 612−617.

(32) Soleymani, L.; Fang, Z.; Sargent, E. H.; Kelley, S. O. *Nat. Nanotechnol.* **2009**, *4*, 844−848.

(33) Soleymani, L.; Fang, Z.; Sun, X.; Yang, H.; Taft, B. J.; Sargent, E. H.; Kelley, S. O. *Angew. Chem.* **2009**, *48*, 8457−8460.

(34) Bin, X.; Sargent, E. H.; Kelley, S. O. *Anal. Chem.* **2010**, *82*, 5928−5931.

(35) Soleymani, L.; Fang, Z.; Lam, B.; Xiaomin, Bin, X.; Vasilyeva, E.; Ross, A. J.; Sargent, E. H.; Kelley, S. O. *ACS Nano* **2011**, *5*, 3360−3366.

(36) Lapierre- Devlin, M. A.; Asher, C. L.; Taft, B. J.; Gasparac, R.; Roberts, M. A.; Kelley, S. O. *Nano Lett.* **2005**, *5*, 1051−1055.

(37) Gasparac, R.; Taft, B. J.; Lapierre-Devlin, M. A.; Lazareck, A. D.; Xu, J. M.; Kelley, S. O. *J. Am. Chem. Soc.* **2004**, *126*, 12270−12271.

(38) Lapierre, M. A.; O'Keefe, M.; Taft, B. J.; Kelley, S. O. *Anal. Chem.* **2003**, *75*, 6327−6333.

(39) Salagierski, M.; Schalken, J. A. *J. Urol.* **2012**, *187*, 795−801.